In conclusion, the present results demonstrate the applicability of 2D-NMR techniques to the elucidation of the proton NMR spectra of ferrocenophanes. Thus, once the basic data are provided by SUPERCOSY and *J*-resolved spectra, additional NOE and decoupling experiments enable the complete assignment of the proton spectra. However, in order to establish the orientation of the S_3 bridge with respect to the protons, it was necessary to use the results from solid-state structures. This combination of techniques provides, for the first time, an unequivocal assignment of the proton NMR spectrum of a ferrocenophane and should provide a basis for future studies.

Acknowledgment. The authors thank the Natural Sciences and Engineering Research Council of Canada for financial support in the form of operating grants to W.R.C., F.G.H., and F.W.B.E.

Supplementary Material Available: Tables of calculated hydrogen atom positions (Tables VII and VIII), anisotropic thermal parameters (Tables IX and X), and data pertaining to mean plane and torsion angles (Tables XI and XII) (9 pages); a table of calculated and observed structure factors (Table XIII) (40 pages). Ordering information is given on any current masthead page.

Contribution from the Department of Chemistry, Rutgers, The State University of New Jersey, New Brunswick, New Jersey 08903, and School of Chemical Sciences, University of Illinois, Urbana, Illinois 61801

Crystal Structure and Magnetic Properties of the Cluster Complex $Cu^{I}_2Cu^{II}_3[(SCH_2CH(CO_2CH_3)NHCH_2-)_2]_3\cdot 2ClO_4\cdot H_2O$, a Mixed-Valence Copper–Mercaptide Species

Parimal K. Bharadwaj,[1a] Elizabeth John,[1a] Chuan-Liang Xie,[1b] Dechun Zhang,[1c] David N. Hendrickson,*[1b] Joseph A. Potenza,*[1a] and Harvey J. Schugar*[1a]

Received June 12, 1986

The synthesis, crystal structure, electronic spectra, magnetic susceptibility (5–300 K), and EPR spectra are reported for the title complex **1**. The complex crystallizes as dark, elongated prisms in space group $P2_1$: a = 11.041 (2) Å, b = 15.820 (3) Å, c = 15.042 (3) Å, β = 98.65 (2)°, Z = 2, and R_F (R_{wF}) = 0.071 (0.073) for 3116 reflections with $I > 2\sigma(I)$. The structure contains discrete $Cu_5[(SCH_2CH(CO_2CH_3)NHCH_2-)_2]_3^{2+}$ clusters with three *cis*-$Cu^{II}N_2S_2$ units arrayed to create triangular S_3 ligation for the two Cu(I) ions. Both perchlorate anions and the water molecule are lattice species. The *cis*-$Cu^{II}N_2S_2$ units of **1** are structurally similar to the remarkably stable $Cu^{II}[(SCH_2CH(CO_2CH_3)NHCH_2-)_2]$ monomer described elsewhere. All three N_2S_2 donor sets exhibit small, similar tetrahedral distortions (18.2, 19.9, and 20.5°) as defined by the dihedral angles between the CuNS planes. Cu(II)–S distances span the range 2.237 (5)–2.266 (4) Å while Cu–N distances range from 1.965 (12) to 2.055 (11) Å. The S–Cu(II)–S, N–Cu(II)–N, and *trans*-N–Cu(II)–S bond angles span the ranges 99.8 (2)–102.2 (2), 83.2 (6)–85.7 (5), and 162.1 (3)–168.3 (4)°, respectively. Both Cu(I) ions exhibit small, comparable displacements (0.129, 0.120 Å) from their approximately triangular S_3 donor sets; Cu(I)–S distances span the range 2.232 (4)–2.291 (5) Å. The S···S contacts within the *cis*-$Cu^{II}N_2S_2$ units (3.459 (6), 3.497 (6), 3.451 (6) Å) are all slightly shorter than the van der Waals contact of 3.7 Å. Effective magnetic moments of **1** per Cu(II) fall in the range 1.74–1.79 μ_B and could be fit to the Kambe model for a triangular cluster having a small isotropic intracluster ferromagnetic exchange interaction (J = 0.26 cm^{-1}) and a TIP of -3.84×10^{-5} cgsu. At X-band frequency, the EPR spectrum of **1** (either polycrystalline or dispersed in a glycol/water glass) consists of an approximately isotropic signal at $g \approx 2.02$. Apparently, the electron-exchange coupling between the three $Cu^{II}N_2S_2$ units occurs at a frequency that exceeds the energy difference represented by the $g_\parallel$ and $g_\perp$ signals exhibited by the isolated *cis*-$Cu^{II}N_2S_2$ monomer. Electronic absorption spectra of **1** are presented and related to those observed for the isolated monomer.

Introduction

We have been interested in synthesizing models of the Cu_A site in cytochrome *c* oxidase. On the basis of published EXAFS data as well as their own detailed EPR and ENDOR studies, Chan and co-workers[2] have suggested that the Cu_A site is a pseudo-tetrahedral $CuN_2(his)S_2(cys)$ unit that has substantial Cu(II)–thiyl radical[3] as opposed to Cu(II)–thiolate character. EPR spectra of the Cu_A site are anomalous in that the *g* values are small (one actually falls below g = 2.00), Cu hyperfine splittings are not resolved, and the relaxation rate is large.[4] Because of the great biochemical significance of cytochrome *c* oxidase, there is considerable interest in preparing stable, paramagnetic model Cu–aliphatic dithiolates that may mimic the atypical spectroscopic signatures of the Cu_A unit. As a first approach at modeling the Cu_A unit, we have prepared a chiral *cis*-$Cu^{II}N_2(cys)S_2(cys)$ chromophore, the ligation of which is supplied by the bridged L-cysteinethiolate species $(^{-}SCH_2CH(CO_2CH_3)NHCH_2-)_2$.[5] The synthesis of this, as well as other, stable *cis*–$Cu^{II}N_2S_2$ chromophores proceeds without appreciable accompanying redox decomposition when macrocyclic tetramines, such as tet a, tet b, and cyclam are displaced from Cu(II) by linear tetradentate amino thiolate ligands such as the above bridged cysteine species, $(HSC(CH_3)_2CH_2NHCH_2-)_2$ or $(HSC(CH_3)_2CH_2NHCH_2-)_2CH_2$. Ligand displacement is accompanied by partial redox decomposition when $Cu(en)_2\cdot 2ClO_4$ or $Cu(H_2O)_6\cdot 2ClO_4$ are used instead of (for example) Cu(tet a)$\cdot 2ClO_4$ as starting materials. The redox decomposition product from the $Cu(en)_2\cdot 2ClO_4$ system is a mixed-valence pentanuclear complex nominally formed from the combination of 3 mol of the $Cu^{II}N_2(cys)S_2(cys)$ monomer with 2 equiv of $Cu^{I}ClO_4$. The synthesis, crystal structure, magnetic properties, EPR spectra, and preliminary electronic absorption spectra of this novel pentanuclear complex (**1**) are reported here. Other reports of mixed-valence Cu(I)/Cu(II) sulfur-bridged polynuclear species include (a) $Cu^{I}_8Cu^{II}_6[SC(CH_3)_2CH_2NH_2]_{12}Cl\cdot 3.5SO_4\cdot{\approx}20H_2O$ (**2**),[6] (b) $Cu^{I}_8Cu^{II}_6[SC(CH_3)_2CH(CO_2)NH_2]_{12}Cl^{5-}$ (**3**), the D-penicillamine analogue of **2**,[7] (c) $Tl_5[Cu^{I}_8Cu^{II}_6(SC(CH_3)_2CO_2)_{12}Cl]\cdot{\approx}12H_2O$ (**4**),[8] (d)

(1) (a) Rutgers University. (b) University of Illinois. (c) Visiting scholar at Rutgers on leave from Division of Chemistry, East China Engineering Institute, Nanjing, Jiangsu, China (PRC).

(2) Stevens, T. H.; Martin, C. T.; Wang, H.; Brudvig, G. W.; Scholes, C. P.; Chan, S. I. *J. Biol. Chem.* **1982**, *257*, 12106.
(3) Peisach, J.; Blumberg, W. E. *Arch. Biochem. Biophys.* **1974**, *165*, 691.
(4) Brudvig, G. W.; Blair, D. F.; Chan, S. I.; *J. Biol. Chem.* **1984**, *259*, 11001.
(5) Bharadwaj, P. K.; Potenza, J. A.; Schugar, H. J. *J. Am. Chem. Soc.* **1986**, *106*, 3151.
(6) Schugar, H. J.; Ou, C.-C.; Thich, J. A.; Potenza, J. A.; Felthouse, T. R.; Haddad, M. S.; Hendrickson, D. N.; Furey, W.; Lalancette, R. A. *Inorg. Chem.* **1980**, *19*, 543.
(7) Birker, P. J. M. W. L.; Freeman, H. C. *J. Am. Chem. Soc.* **1977**, *99*, 6890.
(8) Birker, P. J. M. W. L. *Inorg. Chem.* **1979**, *18*, 3502.

0020-1669/86/1325-4541$01.50/0

and $Cu^{I}_{10}Cu^{II}_{2}[C_4H_5N_2S]_{12}(CH_3CN)_4\cdot 2BPh_4\cdot 4CH_3CN$ (**5**),[9] where $C_4H_5N_2S$ is 1-methyl-2-mercaptoimidazole.

Experimental Section

1. Preparation of the Ligand. A solution of 3 g of *N,N'*-1,2-ethanediylbis(L-cysteine)[10] in 100 mL of dry methanol was saturated with HCl(g) at −5 °C and then heated to 45 °C for 10 h. The resulting dimethyl ester was isolated as the dihydrochloride salt after the solution was reduced to 50 mL and cooled to 25 °C. The white solid (2.9 g, ca. 90% yield) was collected by filtration and dried under vacuum (mp 156–158 °C). ^{1}H NMR (10% DCl, 60 MHz): δ 3.33 (2 H, CH_2, d), 3.68 (2 H, CH_2, s), 3.95 (3 H, CH_3, s), 4.66 (1 H, CH, t).

The free ester was prepared by treating a suspension of the dihydrochloride salt in dry ether with NH_3(g) for 0.5 h. After the solid NH_4Cl was removed by filtration and the solvent evaporated, the free ester was obtained as a colorless, viscous liquid.

2. Preparation of the Title Complex (1). The complex precipitated as a dark, polycrystalline solid when a solution of 0.19 g (5×10^{-4} mol) of $Cu(en)_2\cdot 2ClO_4$ in 10 mL of methanol was added to a solution of 0.18 g (5×10^{-4} mol) of the ligand dihydrochloride in 10 mL of aqueous methanol (50/50 v/v). The solutions were deoxygenated by purging with N_2(g) and filtered through fine glass frits before mixing. Displaced ethylenediamine neutralizes the acid generated when the N_2S_2-donor ligand binds in its free aminodithiolate form to Cu(II). However, it was observed that crystals of the pentanuclear complex better suited for X-ray diffraction studies resulted when the above procedure was repeated with the free ester form of the ligand. The crystalline product was collected by filtration and dried in air (yield: 14%). *Caution!* Compound may explode if heated when dry. Anal. Calcd for $Cu_5[(SCH_2CH(CO_2CH_3)NHCH_2-)_2]_3\cdot 2ClO_4\cdot H_2O$: Cu, 22.40; S, 13.57; C, 25.41; N, 5.93; H, 3.98. Found: Cu, 21.50; S, 14.21; C, 26.50; N, 6.32; H, 4.46.

3. Magnetic Measurements. Variable-temperature (5.0–299.9 K) magnetic susceptibility data were collected with a VTS-50 SQUID susceptometer (S.H.E. Corp.) interfaced with an Apple IIe computer. Measurements were made at 10 kG. Temperature control and measurement were achieved with the S.H.E. digital thermometer control unit, working in conjunction with the computer program CONTROL. Magnetic susceptibility data for $CuSO_4\cdot 5H_2O$ were measured to check the calibration of the susceptometer. A diamagnetism correction of -750×10^{-6} cgsu was calculated from Pascal's constants.[11] This correction was used to calculate the molar paramagnetic susceptibility from the experimental data. The molar paramagnetic susceptibility data were then least-squares fit to the theoretical equation by means of a computer program. EPR spectra of polycrystalline **1** were recorded on a Varian E-9 X-band spectrometer whose frequency was determined by using a Hewlett-Packard Model 5240A digital frequency meter. The magnetic field position was determined with DPPH ($g = 2.0036$).

4. Electronic Spectral Measurements. Electronic spectra were measured by using a Cary 17 spectrophotometer equipped with quartz dewars of standard design.

5. X-ray Diffraction Studies. A crystal of **1** approximately 0.32 × 0.16 × 0.12 mm was mounted on the end of a glass fiber. All diffraction measurements were made by using an Enraf-Nonius CAD-4 diffractometer and Mo Kα radiation. The Enraf-Nonius Structure Determination Package[12] was used for data collection, data processing, and structure solution. Crystal data and additional details of the data collection and refinement are presented in Table I. Intensity data were collected and corrected for decay, absorption (empirical), and *Lp* effects. The systematic absence observed is consistent with two monoclinic space groups, $P2_1$ and $P2_1/m$. Because the N_2S_2 ligand is optically active, the nonchiral space group was rejected. The structure was solved and refined smoothly in space group $P2_1$.

The structure was solved by direct methods[13] and refined on *F* by using full-matrix least-squares techniques. An *E* map based on 350 phases from the starting set with the highest combined figure of merit revealed coordinates for the Cu, S, and N atoms. The remaining non-hydrogen atoms were located from successive difference Fourier maps, each prepared following several cycles of least-squares refinement. Both perchlorate groups were found to be disordered and each was modeled with two O atoms on fully occupied sites and two O atoms on half-occupied sites. The water O atom was located at a logical position with a difference map; it refined smoothly after being added to the model with a multiplier of 0.5. Except for the water molecule, H atoms were added to the model, assuming idealized bond geometry and C–H and N–H distances of 0.95 and 0.87 Å, respectively.[14] H atom temperature factors were set according to $B_H = B_N + 1$ where N is the atom bonded to H. Cu, Cl, S, and N atoms were refined anisotropically. Several cycles of refinement led to convergence with $R_F = 0.071$, $R_{wF} = 0.073$, and GOF = 1.57. Final atomic parameters are listed in Table II. Lists of observed and calculated structure factors, anisotropic thermal parameters, H atom parameters, perchlorate bond distances and angles, and selected bond distances and angles for the thiolate ligands are available.[15]

Table I. Crystal and Refinement Data for **1**

formula	$Cu_5[(SCH_2CH(CO_2CH_3)NHCH_2-)_2]_3\cdot 2ClO_4\cdot H_2O$
fw	1417.8
a, Å	11.041 (2)
b, Å	15.820 (3)
c, Å	15.042 (3)
β, deg	98.65 (2)
V, Å^3	2597 (2)
space group	$P2_1$
Z	2
no. of reflcns used to detn cell const	25 (10.35 < θ < 14.54)
d_{calcd}, g/cm^3	1.813
d_{obsd}, g/cm^3	1.80 (1)
radiation used	graphite monochromated Mo Kα (0.71073 Å)
linear abs coeff, cm^{-1}	24.3
cryst dimens, mm	0.12 × 0.16 × 0.32
rel transmissn factor range	0.90 < *T* < 1.00
diffractometer	Enraf-Nonius CAD-4
data collcn method	θ–2θ
2θ range, deg	2 ≤ 2θ ≤ 50
temp, K	298(1)
scan rate, deg/min	variable
scan range, deg	1.20 + 0.35(tan θ)
weighting scheme[a]	$w = 4(F_o)^2/[\sigma(F_o)^2]^2$
no. of std reflcns	3
% variation in std intens	±1.5%
no. of unique data collcd	4734
no. of data used in refinement	3116 ($F_o^2 \geq 2\sigma(F_o^2)$)
data:parameter ratio	7.9
final GOF[b]	1.57
final R_F,[c] R_{wF}[d]	0.071, 0.073
syst abs obsd	0*k*0, *k* = 2*n* + 1
data collcd	*h*,*k*,±*l*
final largest shift/esd	0.49
highest peak in final diff map, e/Å^3	0.81

[a] $[\sigma(F_o)^2]^2 = [S^2(C + R^2B) + (pF_o^2)^2]/(Lp)^2$, where *S* is the scan rate, *C* is the integrated peak count, *R* is the ratio of scan to background counting time, *B* is the total background count, and *p* is a factor used to downweight intense reflections. For this structure, *p* = 0.04. [b] Error in an observation of unit weight, equal to $[\sum w(|F_o| - |F_c|)^2/(NO - NV)]^{1/2}$ were NO is the number of observations and NV is the number of variables in the least-squares refinement. [c] $R_F = \sum / ||F_o| - |F_c|| / \sum |F_o|$. [d] $R_{wF} = [\sum w(|F_o| - |F_c|)^2/\sum wF_o^2]^{1/2}$.

Description of the Structure

The structure contains discrete $Cu_5[(SCH_2CH(CO_2CH_3)NHCH_2-)_2]_3^{2+}$ cations in which three neutral *cis*-$Cu^{II}N_2S_2$ units are arrayed to create triangular S_3 ligation for two Cu(I) ions. Both perchlorate anions and the single water of hydration are lattice species. A view of the cluster structure and of one component CuN_2S_2 fragment is given in Figure 1, while a simplified view illustrating the basic $Cu_5S_6N_6$ framework is given in Figure

(9) Agnus, Y.; Louis, R.; Weiss, R. *J. Chem. Soc., Chem. Commun.* **1980**, 867.
(10) Blondeau, P.; Berse, C.; Gravel, D. *Can. J. Chem.* **1967**, *45*, 49.
(11) Mulay, L. N. In *Theory and Applications of Molecular Paramagnetism*, Boudreaux, E. A., Mulay, L. N., Eds.; Wiley: New York, 1976; pp 491–6.
(12) Enraf-Nonius Structure Determination Package, Enraf-Nonius: Delft, Holland, 1983.
(13) Main, P.; Fiske, S. J.; Hull, S. E.; Lessinger, L.; Germain, G.; Declercq, J.-P.; Woolfson, M. M. "MULTAN 82. A System of Computer Programs for the Automatic Solution of Crystal Structures from X-ray Diffraction Data"; Universities of York, England, and Louvain, Belgium, 1982.
(14) Churchill, M. R. *Inorg. Chem.* **1973**, *12*, 1213.
(15) Supplementary material.

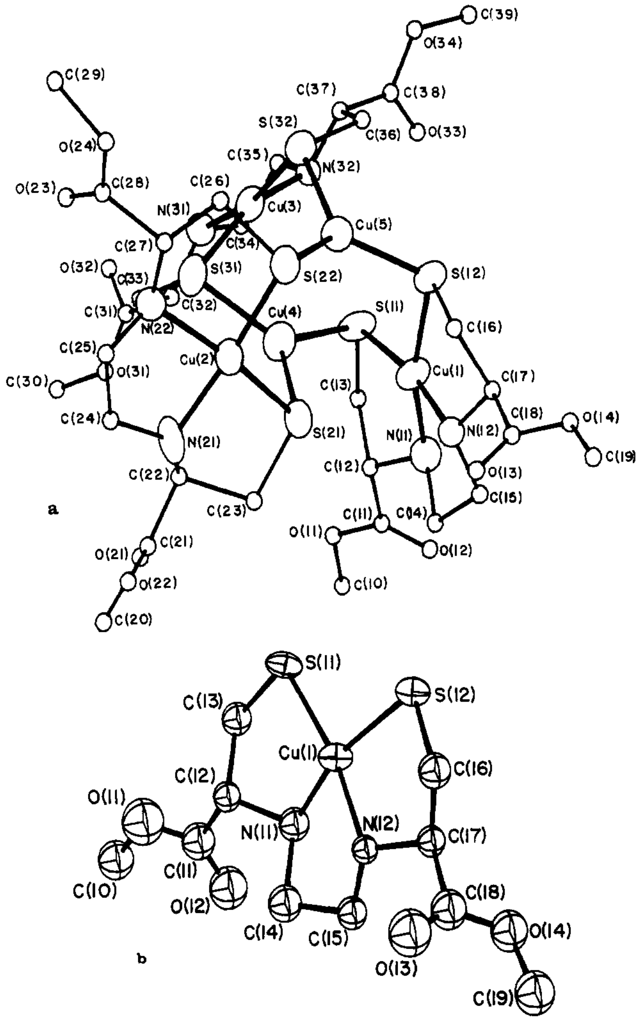

Figure 1. (a) ORTEP view of complex **1** showing the atom-numbering scheme. Boundary ellipses are shown at the 50% probability level. Thermal parameters for the isotropically refined ligand atoms have been set arbitrarily to 1 Å^2. Hydrogen atoms, perchlorate groups, and the lattice water molecule have been omitted for clarity. (b) View of one of the $Cu^{II}N_2S_2$ fragments in **1**.

2. Selected bond distances, bond angles, and other structural details are summarized in Tables III and IV. Four other thiolate-bridged polynuclear Cu(I)/Cu(II) species have been characterized, as noted in the Introduction.[6-9] A unique feature of **1** is that the *cis*-CuN_2S_2 subunits are capable of *independent* existence. Indeed, this monomer has been characterized elsewhere by detailed crystallographic, magnetic, EPR, and electronic-spectral studies[5] and is an unambiguous example of a stable *cis*-$Cu^{II}N_2S_2$ aliphatic dithiolate. Owing to the close similarity of the three *cis*-CuN_2S_2 units of **1** to the reference monomer, we formulate Cu(1), Cu(2), and Cu(3) as Cu(II) species. These Cu(II) ions exhibit small displacements from their respective N_2S_2 donor sets of 0.050, 0.008, and 0.024 Å. The N_2S_2 donor sets show small tetrahedral distortions of 18.2, 19.9, and 20.5°, respectively, as defined by the dihedral angles between the individual CuNS planes; comparable values of 19.0, 20.2, and 21.2° are obtained for the dihedral angles between the CuN_2 and CuS_2 planes. Structural features of the *cis*-$Cu^{II}N_2S_2$ units of the cluster are little changed from those observed for the isolated monomer.[5] Cu(II)–S distances in the cluster range from 2.237 (5) to 2.266 (4) Å whereas those in the monomer are 2.230 (5) and 2.262 (4) Å. Cu(II)–N distances in the cluster span the range 1.965 (12)–2.055 (11) Å while those in the monomer are 2.002 (11) and 2.059 (13) Å. The dihedral angle between the CuS_2 and CuN_2 planes in the monomer is 21.0°. S–Cu(II)–S bond angles vary from 99.8 (2) to 102.2 (2)° and exceed the N–Cu(II)–N values (83.2 (6)–85.7 (5)°). Tetrahedral distortions have reduced

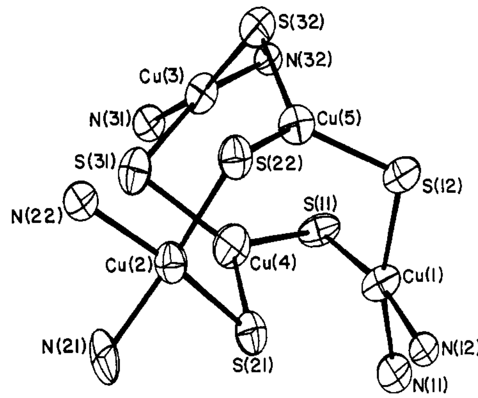

Figure 2. View of the $Cu_5S_6N_6$ cluster framework.

trans-S–Cu–N angles from the ideal value of 180° to about 165 ± 3°. Similar results were observed for the *cis*-$Cu^{II}N_2S_2$ monomer.

Formulation of Cu(4) and Cu(5) as Cu(I) species is in harmony with their approximately triangular S_3Cu coordination geometries. These Cu(I) ions exhibit small displacements (0.129, 0.120 Å) from the S_3 planes. The observed Cu(I)–S distances (range: 2.232 (4)–2.292 (5) Å) are comparable to those noted above for the *cis*-$Cu^{II}N_2S_2$ units. The Cu(5)–S_3 unit is considerably closer to the idealized triangular geometry than is the Cu(4)–S_3 unit, as evidenced by the S–Cu–S angles 119.1 (2)–120.7 (2) and 115.5 (2)–126.5 (2)°, respectively). The $Cu^{I}S_3$ units are nearly parallel (the dihedral angle between the CuS_3 planes is 0.2°) with a Cu(I)···Cu(I) separation of 3.016 (3) Å. Geometrical features of the Cu(I) coordination are similar to those observed for the Cu(I) ions in the $Cu^{I}_8Cu^{II}_6L_{12}Cl$ clusters (L = N_2S_2 or O_2S_2 donor ligand) reported in the literature,[6-9] and for the $Cu^{I}_8L'_{12}$ (L' = chelating 1,1- or 1,2-dithiolate ligand) subunits that are capable of independent existence.[16,17] Similar geometrical parameters also have been reported for the trigonal Cu(I) ions in smaller Cu(I)-thiolate cluster species.[18,19]

The three S···S contacts within the *cis*-$Cu^{II}N_2S_2$ units (Table III) are shorter than the van der Waals contact of 3.7 Å, but not nearly as short as those reported (2.734 (1)–2.821 (2) Å) for Mo(VI) complexes with $O_2N_2S_2$ donor sets.[20] While the extent of partial disulfide bond formation in **1** is small, weakly interacting sulfur centers may give rise to conspicuous spectroscopic effects.[21]

Structural parameters for the ligand, disordered perchlorate anions, and the lattice water molecule are not unusual and are included as supplementary material.

Magnetic Susceptibility

Magnetic exchange within the cluster was probed from the perspective of the Kambe model for trimers exhibiting isotropic exchange ($J_{12} = J_{13} = J_{23} = J$) or anisotropic exchange ($J_{12} = J_{13} = J$; $J_{23} = J'$).[22] Expressions for the magnetic susceptibility are given by eq 1 and 2, respectively, for the two models. Ex-

$$\chi_M = [Ng^2\beta^2/4kT][(1 + 5e^x)/(1 + e^x)] \qquad x = 3J/2kT \tag{1}$$

$$\chi_M = \left(\frac{Ng^2\beta^2}{4kT}\right)\left(\frac{e^{-3J'/2kT} + e^{(-4J + J')/2kT} + 10e^{(2J + J')/2kT}}{e^{-3J'/2kT} + e^{(-4J + J')/2kT} + 2e^{(2J + J')/2kT}}\right) \tag{2}$$

perimental magnetic susceptibility data were corrected for the

(16) McCandlish, L. E.; Bissell, E. C.; Coucouvanis, D.; Fackler, J. P.; Knox, K. *J. Am. Chem. Soc.* **1968**, *90*, 7357.
(17) Hollander, F. J.; Coucouvanis, D. *J. Am. Chem. Soc.* **1974**, *96*, 5646.
(18) Dance, I. G.; Calabrese, J. C. *Inorg. Chim. Acta* **1976**, *19*, L41.
(19) Dance, I. G. *Aust. J. Chem.* **1978**, *31*, 2195.
(20) Berg, J. M.; Spira, D. J.; Hodgson, K. O.; Bruce, A. E.; Miller, K. F.; Corbin, J. L.; Stiefel, E. I. *Inorg. Chem.* **1984**, *23*, 3412 and references cited therein.
(21) Stein, C. A.; Taube, H. *J. Am. Chem. Soc.* **1978**, *100*, 1635.
(22) Sinn, E. *Coord. Chem. Rev.* **1970**, *5*, 313.

Table II. Fractional Atomic Coordinates and Thermal Parameters for **1**

	x	y	z	B or B_{eq},[a] Å^2		x	y	z	B or B_{eq},[a] Å^2
Cu(1)	0.2716 (2)	0.000	0.6278 (1)	3.54 (5)	O(34)	−0.096 (1)	0.2540 (8)	0.8883 (8)	4.2 (3)*
Cu(2)	0.4601 (2)	−0.1915 (2)	0.8626 (1)	3.21 (5)	N(11)	0.206 (1)	−0.049 (1)	0.5068 (9)	4.3 (4)
Cu(3)	0.0519 (2)	−0.0617 (2)	0.8895 (1)	3.08 (4)	N(12)	0.437 (1)	0.0004 (9)	0.5837 (8)	3.1 (3)
Cu(4)	0.2060 (2)	−0.1277 (2)	0.7615 (2)	4.39 (6)	N(21)	0.467 (1)	−0.314 (1)	0.828 (1)	4.3 (4)
Cu(5)	0.3439 (2)	0.0151 (2)	0.8641 (1)	3.38 (5)	N(22)	0.473 (1)	−0.2386 (9)	0.9864 (9)	3.2 (3)
Cl(1)	0.1426 (5)	0.4723 (6)	0.8956 (4)	8.8 (2)	N(31)	−0.098 (1)	−0.1395 (9)	0.8635 (9)	3.3 (3)
Cl(2)	0.3134 (8)	0.2555 (7)	0.4381 (4)	11.7 (3)	N(32)	−0.061 (1)	0.0293 (9)	0.8417 (8)	3.0 (3)
S(11)	0.0904 (4)	−0.0296 (3)	0.6745 (3)	3.7 (1)	C(10)	−0.085 (2)	−0.241 (2)	0.351 (2)	7.6 (7)*
S(12)	0.3528 (4)	0.0884 (3)	0.7385 (3)	3.5 (1)	C(11)	0.042 (2)	−0.143 (1)	0.425 (1)	5.4 (5)*
S(21)	0.3904 (4)	−0.1603 (3)	0.7176 (3)	3.6 (1)	C(12)	0.109 (2)	−0.115 (1)	0.515 (1)	3.8 (4)*
S(22)	0.5047 (4)	−0.0637 (3)	0.9222 (3)	3.6 (1)	C(13)	0.017 (2)	−0.078 (1)	0.571 (1)	4.3 (4)*
S(31)	0.1724 (4)	−0.1771 (4)	0.8986 (3)	3.8 (1)	C(14)	0.313 (2)	−0.080 (1)	0.464 (1)	4.5 (4)*
S(32)	0.1918 (4)	0.0367 (3)	0.9443 (3)	3.5 (1)	C(15)	0.410 (2)	−0.015 (1)	0.482 (1)	3.8 (4)*
O(W)[b]	0.045 (4)	0.086 (3)	0.396 (3)	12 (1)*	C(16)	0.513 (2)	0.077 (1)	0.714 (1)	3.7 (4)*
O(1)	0.075 (3)	0.475 (2)	0.812 (2)	16.6 (9)*	C(17)	0.507 (2)	0.072 (1)	0.613 (1)	3.5 (4)*
O(2′)[b]	0.243 (4)	0.509 (3)	0.904 (3)	11 (1)*	C(18)	0.641 (2)	0.066 (1)	0.592 (1)	4.6 (4)*
O(2)[b]	0.197 (3)	0.557 (2)	0.933 (2)	6.4 (7)*	C(19)	0.806 (2)	0.138 (2)	0.551 (2)	6.3 (6)*
O(3)	0.056 (2)	0.472 (2)	0.948 (2)	13.2 (7)*	C(20)	0.261 (2)	−0.530 (2)	0.642 (2)	7.1 (6)*
O(4′)[b]	0.246 (3)	0.441 (3)	0.852 (2)	10 (1)*	C(21)	0.376 (2)	−0.420 (1)	0.715 (1)	5.2 (5)*
O(4)	0.167 (3)	0.396 (2)	0.947 (2)	6.8 (8)*	C(22)	0.375 (1)	−0.336 (1)	0.754 (1)	2.8 (3)*
O(5′)[b]	0.302 (4)	0.287 (3)	0.515 (3)	12 (1)*	C(23)	0.378 (2)	−0.268 (1)	0.673 (1)	4.6 (4)*
O(5)[b]	0.278 (4)	0.191 (3)	0.484 (3)	10 (1)*	C(24)	0.476 (2)	−0.365 (1)	0.903 (1)	5.1 (5)*
O(6′)[b]	0.182 (4)	0.286 (3)	0.401 (3)	10 (1)*	C(25)	0.527 (2)	−0.321 (1)	0.988 (1)	4.9 (5)*
O(6)[b]	0.356 (4)	0.180 (3)	0.391 (3)	11 (1)*	C(26)	0.483 (2)	−0.093 (1)	1.037 (1)	3.8 (4)*
O(7)	0.440 (3)	0.305 (2)	0.472 (2)	17 (1)*	C(27)	0.525 (2)	−0.182 (1)	1.058 (1)	3.6 (4)*
O(8)	0.298 (2)	0.266 (2)	0.361 (2)	15[c]	C(28)	0.490 (2)	−0.212 (1)	1.149 (1)	4.4 (4)*
O(11)	−0.019 (1)	−0.210 (1)	0.433 (1)	7.1 (4)*	C(29)	0.513 (2)	−0.185 (2)	1.305 (2)	7.5 (6)*
O(12)	0.056 (2)	−0.111 (1)	0.357 (1)	8.0 (4)*	C(30)	−0.219 (2)	−0.425 (2)	0.788 (2)	6.4 (6)*
O(13)	0.696 (1)	0.004 (1)	0.605 (1)	7.4 (4)*	C(31)	−0.166 (2)	−0.287 (1)	0.827 (1)	4.0 (4)*
O(14)	0.678 (1)	0.1382 (9)	0.5665 (9)	5.4 (3)*	C(32)	−0.066 (2)	−0.221 (1)	0.830 (1)	3.6 (4)*
O(21)	0.267 (1)	−0.4430 (9)	0.6712 (9)	5.5 (3)*	C(33)	0.048 (2)	−0.255 (1)	0.884 (1)	4.1 (4)*
O(22)	0.466 (1)	−0.464 (1)	0.7219 (9)	6.4 (4)*	C(34)	−0.194 (2)	−0.089 (1)	0.808 (1)	3.5 (4)*
O(23)	0.408 (1)	−0.258 (1)	1.153 (1)	6.6 (4)*	C(35)	−0.188 (2)	−0.001 (1)	0.841 (1)	4.0 (4)*
O(24)	0.549 (1)	−0.171 (1)	1.2150 (9)	6.6 (4)*	C(36)	0.103 (2)	0.128 (1)	0.895 (1)	4.3 (4)*
O(31)	−0.141 (1)	−0.353 (1)	0.7849 (9)	5.9 (3)*	C(37)	−0.033 (2)	0.112 (1)	0.886 (1)	3.5 (4)*
O(32)	−0.258 (1)	−0.2764 (9)	0.8609 (9)	5.3 (3)*	C(38)	−0.100 (2)	0.185 (1)	0.842 (1)	3.5 (4)*
O(33)	−0.150 (1)	0.1842 (9)	0.7604 (8)	5.0 (3)*	C(39)	−0.147 (2)	0.329 (1)	0.845 (1)	5.0 (5)*

[a] Estimated standard deviations are given in parentheses. Starred values denote atoms that were refined isotropically. For anisotropically refined atoms, the equivalent isotropic thermal parameter, B_{eq}, is given where $B_{eq} = {}^4/_3[a^2B_{11} + b^2B_{22} + c^2B_{33} + ab(\cos\alpha)B_{12} + ac(\cos\beta)B_{13} + bc(\cos\gamma)B_{23}]$. [b] For these atoms, the atom multiplier was set equal to 0.5. [c] The thermal parameter for the perchlorate oxygen atom O(8) showed large fluctuations and was held constant at 15 Å^2 for the final cycles of refinement.

diamagnetism of **1** and fit by least-squares to eq 1 and 2. The temperature dependence of the susceptibilities and magnetic moments indicate a small ferromagnetic interaction, which may be modeled equally well by either equation. Agreement between the experimental values (solid curves) and values calculated by using eq 1 (open circles) for $J = 0.26$ cm^{-1} and TIP = -3.84×10^{-5} cgsu is illustrated in Figure 3. Fitting of the data to eq 2 yields the corresponding parameters $J = 1.51$ cm^{-1}, $J' = -0.57$ cm^{-1}, and TIP = -7.24×10^{-5} cgsu.

The EPR spectra of **1** (not shown) consist of an approximately isotropic signal at $g = 2.02$ for both the polycrystalline material (298, 80 K) and the solution complex in a glycerol/H_2O glass at 80 K. The magnetic susceptibility data support the structural result that three of the five Cu ions are in the divalent state and that the Cu(II) ions exhibit a weak ferromagnetic intracluster interaction. However, owing to the weak nature of the coupling, the $S' = {}^3/_2$ ground state is not substantially populated (the magnetic moment per Cu(II) at 5.00 K is only 1.74 μ_B. The observed ferromagnetic interactions may be transmitted via a S–Cu(I)–S superexchange pathway. Such a path is predicted to yield net ferromagnetic exchange owing to orthogonality of the orbitals centered at the trigonally hybridized Cu(I) ions.

The structural results show that the three *cis*-$Cu^{II}N_2S_2$ units have different orientations (see Figure 2). In the absence of exchange coupling, each of these approximately planar Cu(II) chromophores might be expected to exhibit a $g_\parallel$ signal and one or two $g_\perp$ signals. Since the *cis*-$Cu^{II}N_2S_2$ units are so similar crystallographically, only a single $g_\parallel$ signal and one or two $g_\perp$ signals would be expected for **1**. The observed, approximately isotropic signal for **1** implies that these signals are exchange-averaged; i.e., the frequency of electron exchange among the

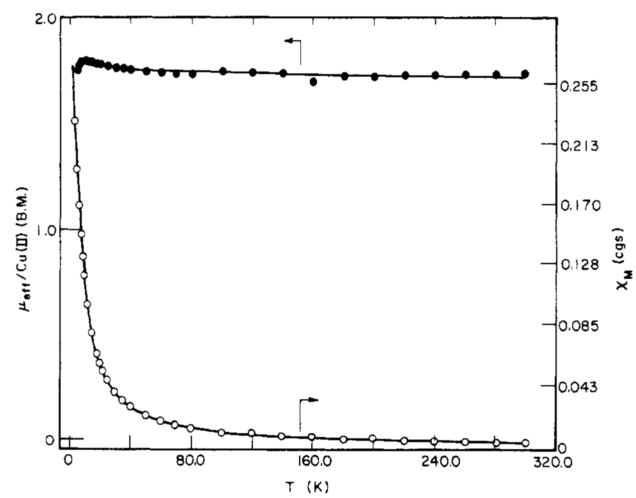

Figure 3. Experimental molar paramagnetic susceptibility per cluster and effective magnetic moment per Cu(II) ion in the pentanuclear complex **1** vs. temperature. The solid line represents the least-squares fit to eq 1 with $J = 0.26$ cm^{-1} and a TIP of -3.84×10^{-5} cgsu; solid and open circles give the experimental data.

Cu(II) sites is greater than the energy difference represented by the $g_\parallel$ and $g_\perp$ values. Moreover, the isotropic EPR spectra observed for **1** in glycerol/water glass indicate that the cluster remains intact in that medium and that the dominant, albeit weak, ferromagnetic interaction is intracluster rather than intercluster in origin. In contrast, the well-characterized, isolated *cis*-$Cu^{II}N_2S_2$

Table III. Selected Bond Distances (Å) and Angles (deg) in **1**

		Coordination Sphere			
Cu(1)–S(11)	2.266 (4)	Cu(2)–S(21)	2.256 (4)	Cu(3)–S(31)	2.251 (5)
Cu(1)–S(12)	2.255 (4)	Cu(2)–S(22)	2.237 (5)	Cu(3)–S(32)	2.259 (4)
Cu(1)–N(11)	2.007 (13)	Cu(2)–N(21)	2.015 (14)	Cu(3)–N(31)	2.055 (11)
Cu(1)–N(12)	2.034 (11)	Cu(2)–N(22)	1.991 (12)	Cu(3)–N(32)	1.965 (12)
S(11)–C(13)	1.81 (2)	S(21)–C(23)	1.83 (2)	S(31)–C(33)	1.84 (2)
S(12)–C(16)	1.87 (2)	S(22)–C(26)	1.84 (2)	S(32)–C(36)	1.83 (2)
N(11)–C(12)	1.51 (2)	N(21)–C(22)	1.44 (2)	N(31)–C(32)	1.44 (2)
N(11)–C(14)	1.51 (2)	N(21)–C(24)	1.38 (2)	N(31)–C(34)	1.48 (2)
N(12)–C(15)	1.53 (2)	N(22)–C(25)	1.44 (2)	N(32)–C(35)	1.49 (2)
N(12)–C(17)	1.41 (2)	N(22)–C(27)	1.45 (2)	N(32)–C(37)	1.49 (2)
Cu(4)–S(11)	2.291 (5)	Cu(4)–S(31)	2.287 (4)	Cu(5)–S(22)	2.238 (4)
Cu(4)–S(21)	2.291 (5)	Cu(5)–S(12)	2.232 (4)	Cu(5)–S(32)	2.235 (4)
		Cu(II)–Cu(I)			
Cu(1)···Cu(4)	3.015 (3)	Cu(3)···Cu(4)	2.946 (3)	Cu(2)···Cu(5)	3.514 (3)
Cu(2)···Cu(4)	3.149 (3)	Cu(1)···Cu(5)	3.532 (2)	Cu(3)···Cu(5)	3.519 (2)
		Cu(II)···Cu(II)			
Cu(1)···Cu(2)	4.876 (3)	Cu(1)···Cu(3)	5.020 (2)	Cu(2)···Cu(3)	5.024 (3)
		S···S			
S(11)···S(12)	3.459 (6)	S(21)···S(22)	3.497 (6)	S(31)···S(32)	3.451 (6)
		Cu(I)···Cu(I)			
		Cu(4)···Cu(5)	3.016 (3)		
S(11)–Cu(1)–S(12)	99.8 (2)	S(21)–Cu(2)–S(22)	102.2 (2)	S(31)–Cu(3)–S(32)	99.8 (2)
S(11)–Cu(1)–N(11)	89.3 (4)	S(21)–Cu(2)–N(21)	89.0 (4)	S(31)–Cu(3)–N(31)	88.7 (4)
S(11)–Cu(1)–N(12)	168.3 (4)	S(21)–Cu(2)–N(22)	162.4 (3)	S(31)–Cu(3)–N(32)	162.1 (3)
S(12)–Cu(1)–N(11)	162.9 (4)	S(22)–Cu(2)–N(21)	163.8 (4)	S(32)–Cu(3)–N(31)	165.9 (4)
S(12)–Cu(1)–N(12)	87.8 (3)	S(22)–Cu(2)–N(22)	89.0 (4)	S(32)–Cu(3)–N(32)	89.3 (4)
N(11)–Cu(1)–N(12)	85.7 (4)	N(21)–Cu(2)–N(22)	83.2 (6)	N(31)–Cu(3)–N(32)	85.5 (5)
S(11)–Cu(4)–S(21)	115.5 (2)	S(21)–Cu(4)–S(31)	117.1 (2)	S(12)–Cu(5)–S(32)	120.7 (2)
S(11)–Cu(4)–S(31)	126.5 (2)	S(12)–Cu(5)–S(22)	119.1 (2)	S(22)–Cu(5)–S(32)	119.4 (2)
Cu(1)–S(11)–Cu(4)	82.8 (1)	Cu(2)–S(21)–Cu(4)	87.7 (2)	Cu(3)–S(31)–Cu(4)	80.9 (2)
Cu(1)–S(12)–Cu(5)	103.8 (2)	Cu(2)–S(22)–Cu(5)	103.5 (2)	Cu(3)–S(32)–Cu(5)	103.1 (2)
Cu(1)–S(11)–C(13)	97.2 (5)	Cu(2)–S(21)–C(23)	98.5 (6)	Cu(3)–S(31)–C(33)	96.6 (6)
Cu(1)–S(12)–C(16)	94.2 (5)	Cu(2)–S(22)–C(26)	95.5 (5)	Cu(3)–S(32)–C(36)	95.7 (6)
Cu(4)–S(11)–C(13)	110.0 (6)	Cu(4)–S(21)–C(23)	107.1 (6)	Cu(4)–S(31)–C(33)	110.1 (5)
Cu(5)–S(12)–C(16)	106.3 (5)	Cu(5)–S(22)–C(26)	107.5 (5)	Cu(5)–S(32)–C(36)	107.6 (6)
Cu(1)–N(11)–C(12)	110.8 (9)	Cu(2)–N(21)–C(22)	112.4 (9)	Cu(3)–N(31)–C(32)	111.1 (9)
Cu(1)–N(11)–C(14)	108.3 (9)	Cu(2)–N(21)–C(24)	110 (1)	Cu(3)–N(31)–C(34)	105.5 (9)
Cu(1)–N(12)–C(15)	106.2 (8)	Cu(2)–N(22)–C(25)	109 (1)	Cu(3)–N(32)–C(35)	108.2 (9)
Cu(1)–N(12)–C(17)	112.3 (9)	Cu(2)–N(22)–C(27)	115.6 (9)	Cu(3)–N(32)–C(37)	114.2 (9)

Table IV. Least-Squares Planes and Selected Dihedral Angles in **1**

Displacement of Atoms[a] from Mean Plane, Å

plane I		plane II		plane III		plane IV		plane V	
N(11)	0.28 (2)	N(21)	0.30 (2)	N(31)	−0.31 (2)	S(11)	0.0	S(12)	0.0
N(12)	−0.27 (2)	N(22)	−0.30 (2)	N(32)	0.31 (1)	S(21)	0.0	S(22)	0.0
S(11)	−0.22 (1)	S(21)	−0.22 (1)	S(31)	0.24 (1)	S(31)	0.0	S(32)	0.0
S(12)	0.22 (1)	S(22)	0.22 (1)	S(32)	−0.25 (1)	Cu(4)*	0.129 (3)	Cu(5)*	0.120 (3)
Cu(1)*	−0.050 (1)	Cu(2)*	0.008 (2)	Cu(3)*	−0.024 (2)				

Dihedral Angles, deg

planes I/II	76.5	Cu(1)–S(11)–N(11)/Cu(1)–S(12)–N(12)	18.2
plane I/III	68.1	Cu(2)–S(21)–N(21)/Cu(2)–S(22)–N(22)	19.9
planes II/III	64.2	Cu(3)–S(31)–N(31)/Cu(3)–S(32)–N(32)	20.5
planes IV/V	0.2		

[a] Starred atoms were not used to define the plane.

monomer does exhibit unmistakably anisotropic EPR spectra as (a) a polycrystalline species, (b) a dopant in a diamagnetic host *cis*-$Ni^{II}N_2S_2$ lattice, and (c) a species in a frozen DMF matrix.[5]

Electronic Spectra

The electronic spectra of **1** in glassed glycerol/DMF at 80 K are presented in Figure 4. Not shown are the room-temperature spectra, which are significantly less well resolved. Owing to the substantial structural differences between the $Cu^{I}S_3$ and $Cu^{II}N_2S_2$ metal sites in this pentanuclear complex, *low-energy* mixed-valence transitions are not expected. This expectation is realized by the absence of electronic absorption over the 750–1500-nm region. The three lowest energy absorptions of the pentanuclear complex appear to be red-shifted analogues of those exhibited by the isolated $Cu^{II}N_2S_2$ monomer. The lowest energy absorption at ≈620 nm ($\epsilon \approx 800$ M^{-1} cm^{-1} per Cu(II)) may be assigned as the LF band of the *cis*-$Cu^{II}N_2S_2$ units, possibly enhanced due to "intensity stealing" from the strong near-UV absorptions. The monomeric $Cu^{II}N_2S_2$ complex exhibits a comparably intense LF absorption at ≈545 nm. The absorptions at ≈388 and ≈460 nm have energies and an intensity ratio appropriate for σ- and π-(thiolate) → Cu(II) LMCT, respectively. Apparently analogous absorptions are present in the spectra of the monomer at ≈330 and ≈390 nm, respectively. These near-UV absorptions in the spectra of the monomer and **1** are separated by comparable amounts (≈4000 cm^{-1}). Moreover, as would be predicted for

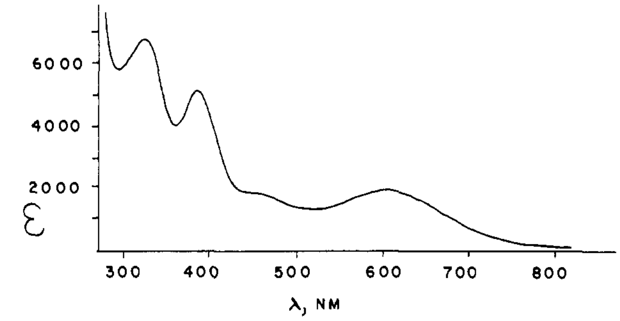

Figure 4. Electronic absorption spectra of **1** in glassed glycerol/DMF (3:1) at 80 K.

LMCT, the near-UV absorptions and the LF absorption (a measure of the shift in the Cu(II) HOMO) of **1** all shift in the same direction relative to the monomer. Other workers have reported that σ(thiolate) → Co(III) LMCT is not significantly shifted by the additional ligation of thiolate to either Ag(I) or CH_3Hg^+.[23] However, adduct formation resulted in the relatively small decreases in the average ligand field of the $Co^{III}N_5S$ and $Co^{III}N_4OS$ chromophores. Monomer spectra in DMF at 80 K do not contain a high-energy absorption corresponding to the intense band at ≈327 nm for **1**. This additional absorption in **1** therefore, is presumably associated with the Cu(I) sites. An absorption at ≈365 nm has been attributed to the Cu(I)–thiolate sites of a mixed-valence, mixed-metal Cu(I)–Co(III) tetramer and assigned as Cu(I) → S(thiolate) MLCT.[24] We wish to refrain from analyzing the spectra of **1** further until the electronic structure of the monomer becomes established. Toward this end, a combination of molecular orbital[25] and detailed spectroscopic studies of the monomer are being pursued.

Acknowledgment. Research at Rutgers was supported in part by the NSF (Grant CHE-8417548) and the David and Johanna Busch Foundation. The X-ray diffraction/crystallographic computing facility at Rutgers was purchased with NIH Grant 1510 RRO 1486 01A1. Research at the University of Illinois was supported by the National Institutes of Health (Grant HL13652).

Supplementary Material Available: Tables of anisotropic thermal parameters, hydrogen atom parameters, bond distances and angles for the $[(SCH_2CH(CO_2CH_3)NHCH_2-)_2]$ ligands and perchlorate groups, and calculated and experimental magnetic susceptibility data (5 pages); a table of observed and calculated structure factors (16 pages). Ordering information is given on any current masthead page.

(23) Heeg, M. J.; Elder, R. C.; Deutsch, E. *Inorg. Chem.* **1979**, *18*, 2036.

(24) Lane, R. H.; Pantaleo, N. S.; Farr, J. K.; Coney, W. M.; Newton, M. G. *J. Am. Chem. Soc.* **1978**, *100*, 1610 and references cited therein.

(25) Westbrook, J.; Krogh-Jespersen, K., unpublished results.

Contribution from the Department of Chemistry, Purdue University, West Lafayette, Indiana 47907

Multiply Bonded Octahalodiosmate(III) Anions. 3.[1] Synthesis and Characterization of the Octahalodiosmate(III) Anions $[Os_2X_8]^{2-}$ (X = Cl, Br). Crystal Structure Determinations of Two Forms of $(PPN)_2Os_2Cl_8$ (PPN = Bis(triphenylphosphine)nitrogen(1+))

Phillip E. Fanwick, Stephen M. Tetrick, and Richard A. Walton*

Received August 19, 1986

The triply bonded octahalodiosmate(III) anions $[Os_2X_8]^{2-}$ (X = Cl, Br) are formed by the reactions of the diosmium(III) carboxylates $Os_2(O_2CR)_4Cl_2$ (R = CH_3, n-C_3H_7) with gaseous HX in ethanol and have been isolated as their n-Bu_4N, Ph_4As, and PPN (bis(triphenylphosphine)nitrogen(1+)) salts. These complexes are essentially diamagnetic, they behave as 1:2 electrolytes in acetonitrile, and they have IR and electronic absorption spectra that accord with this formulation. Their electrochemical properties (cyclic voltammetry in 0.1 M TBAH–CH_2Cl_2) reveal the existence of an accessible one-electron oxidation ($E_{p,a} \simeq +1.1$ V vs. Ag/AgCl) and an irreversible one-electron reduction at $E_{p,c} \simeq -0.9$ V vs. Ag/AgCl. These anions are believed to have the $\sigma^2\pi^4\delta^2\delta^{*2}$ ground-state electronic configuration; since there is no net δ component to the Os–Os bonding, free rotation of the OsX_4 units about the Os–Os bond can occur. In accord with this expectation, two crystalline forms of $(PPN)_2Os_2Cl_8$ have been isolated from CH_2Cl_2–diethyl ether solutions, one green (**1**) and the other brown (**2**), in which different rotational geometries are encountered. The crystal data for **1** at −190 °C are as follows: space group $P2_1/c$; a = 23.167 (4) Å; b = 13.423 (4) Å; c = 22.867 (5) Å; β = 107.80 (3)°; V = 6771 (6) Å^3; Z = 4. For **2**, the crystal data at 22 °C are as follows: space group $C2/c$; a = 33.415 (6) Å; b = 13.692 (2) Å; c = 21.634 (4) Å; V = 6798 (5) Å^3; Z = 4. In both structures a disorder is present that is of a type encountered in other $[M_2X_8]^{n-}$ species, in which the Os–Os unit is randomly present in two orientations with the major orientation having an occupancy of ca. 70% for both **1** and **2**. The Os–Os distance is very short in **1** and **2**, viz., 2.206 (1) and 2.212 (1) Å for the major orientation, respectively. In **1** the disorder is such that there are two different staggered rotational geometries for the major and minor orientations (χ = 11.4 [8] and 39.8 [14]°, respectively), while for **2** the $[Os_2Cl_8]^{2-}$ units are rigorously eclipsed. These results indicate that, for the $[Os_2Cl_8]^{2-}$ anion, crystal-packing forces rather than nonbonded Cl···Cl repulsions dictate the rotational geometry.

Introduction

In the development of multiple metal–metal bond chemistry, the notion of isoelectronic relationships between dimetal cores has helped in the expansion of this field to different metals. For example, such reasoning led to persistent, and eventually successful, attempts to isolate complexes of the quadruply bonded $(W\overset{4}{-}W)^{4+}$ core that were isoelectronic with those of Re_2^{6+} and Mo_2^{4+}.[2,3] Among the important classes of such complexes are homoleptic halide anions of the type $[M_2X_8]^{n-}$ (X = F, Cl, Br, I). These species have been found to possess metal–metal bond orders of

(1) Part 2: Agaskar, P. A.; Cotton, F. A.; Dunbar, K. R.; Falvello, L. R.; Tetrick, S. M.; Walton, R. A. *J. Am. Chem. Soc.* **1986**, *108*, 4850.

(2) (a) Cotton, F. A.; Walton, R. A. *Multiple Bonds between Metal Atoms*; Wiley: New York, 1982. (b) Cotton, F. A.; Walton, R. A. *Struct. Bonding (Berlin)* **1985**, *62*, 1.

(3) Sattelberger, A. P.; McLaughlin, K. W.; Huffman, J. C. *J. Am. Chem. Soc.* **1981**, *103*, 2880.

0020-1669/86/1325-4546$01.50/0